DOI 10.15622/ia.23.2.7

D. BALONI, D. RAI, P. SIVAGAMINATHAN, H. ANANDARAM, M. THAPLIYAL, K. JOSHI

H-DETECT: AN ALGORITHM FOR EARLY DETECTION OF HYDROCEPHALUS

Baloni D., Rai D., Sivagaminathan P., Anandaram H., Thapliyal M., Joshi K. **H-Detect: an Algorithm for Early Detection of Hydrocephalus.**

Abstract. Hydrocephalus is a central nervous system disorder which most commonly affects infants and toddlers. It starts as an abnormal build-up of cerebrospinal fluid in the ventricular system of the brain. Hence, early diagnosis becomes vital, which may be performed by Computed Tomography (CT), one of the most effective diagnostic methods for diagnosing Hydrocephalus (CT), where the enlarged ventricular system becomes apparent. However, most disease progression assessments rely on the radiologist's evaluation and physical measures, which are subjective, time-consuming, and inaccurate. This paper develops an automatic prediction utilizing the H-detect framework for enhanced accurate hydrocephalus prediction. This paper uses a pre-processing step to normalize the input image and remove unwanted noises, which can help extract valuable features easily. The feature extraction is done by segmenting the image based on edge detection using triangular fuzzy rules. Thereby, the exact information on the nature of CSF inside the brain is highlighted. These segmented images are saved and again given to the CatBoost algorithm. The Categorical feature processing allows for quicker training. When necessary, the overfitting detector will stop model training and thus efficiently predicts Hydrocephalus. The outcomes demonstrate that the new H-detect strategy outperforms the traditional approaches.

Keywords: Hydrocephalus, Computed Tomography (CT), H-detect technique, Cerebrospinal fluid (CSF), Triangular fuzzy rules, Edge detect.

1. Introduction. Hydrocephalus is a typical central nervous system disorder engendered by abnormalities in Cerebrospinal Fluid (CSF) circulation. It is caused by an aberrant development of dynamic CSF balance inside the brain's ventricular system [1]. As a result, the ventricles bulge and compress the surrounding brain tissue, resulting in potentially dangerous intracranial hypertension. The degree of ventricular enlargement is frequently considerable, necessitating neurosurgery. It has some of the most severe conditions affecting the central nervous system in children and calls for early neurosurgical treatment [2]. Although this disorder can affect patients of any age, it most commonly affects newborns and babies in their early period of living. Hydrocephalus is predicted to affect one out of every 500 newborns [3]. Hydrocephalus has been examined and scanned; nevertheless, there is no standard solution or efficient strategy for the precise detection and quantitative assessment. Existing measuring methods are predominantly qualitative and produce unsatisfactory results [4]. Radiological methods, such as Computer Tomography (CT) and Magnetic Resonance Imaging (MRI), play a major role in the evaluation of Hydrocephalus (MRI). These tests yield three-dimensional (3D), volumetric

pictures of the brain. However, Hydrocephalus is still primarily assessed manually. It is often based on a qualitative study of the lesion size and other distinguishing characteristics [5].

These methods and procedures use various biophysical factors to depict anatomical features and pathological changes in the human brain. The advancement of medical imaging technology can significantly improve the identification and treatment of numerous lesions and pathological alterations [6]. Radiological diagnostics enable the precise identification of the lesion. A comprehensive analysis of the condition is required before making a treatment approach. The development of tools for automated pathogenic change recognition and classification is thus one of the trickiest problems in contemporary clinical image processing and analysis [7]. There are several methods for segmenting the CSF and the brain ventricular system from CT and MRI imaging. However, only a few papers have been undertaken regarding image processing and analysis in the quantitative assessment of Hydrocephalus [8]. These works are typically significant, and there has been no comprehensive research in this field. It is difficult because of the intricacy and wide range of brain regions. As a result, most known algorithms are based on manual or semi-manual CSF extraction or automated segmentation utilizing basic image processing methods [9].

As a result, this paper aims to propose an H-detect framework which aims:

– To remove the noise existing in the raw data and normalize that can be understandable by the model developed.

– To develop an edge detection using a triangular fuzzy rules model for a significant feature extraction process that can contribute highly to a better understanding of the predicting algorithm.

– To utilize the efficient CatBoost algorithm that can learn the extracted features and predict the disease, thereby improving the accuracy of hydrocephalus diagnosis.

This essay is divided into five distinct sections: Section 1, which discusses the introduction of the research; Section 2, which highlights earlier work completed with the same goal; Section 3, which elaborates the proposed method with three subsections; Section 4, which discusses the implementation of the model and the findings achieved; and Section 5, which wraps up the essay.

2. Literature Survey. In paper [10] analysis of the DL-based MRI image recognition system for bone fracture diagnosis. The study demonstrated that the MRI pictures could be categorised and arranged using deep convolutional neural networks. The CNN was able to gather

information at a high rate and was not hindered by the surrounding tissues of the hydrocephalus when collecting the 3D images of the hydrocephalus. The research still has significant drawbacks, such as the fact that deep learning depends on data.

According to the authors in [11], convolutional neural networks were used to extract patient-specific information from pictures, create dimensions for the lesion location in the picture, and apply a predetermined recognition system. Besides a classifier, the questionable components were categorised. The properties of the conventional physically constructed identification entity were altered by a small modification to the recognition system. The deep convolutional network can precisely identify the lesion's site and has a wealth of characteristics. But still, there is a need to enhance the accuracy of the paper by utilizing the data from the features in an efficient manner.

Convolutional network segment brain MRI semantic pictures were employed by the authors in [12]. In accordance with the findings, the brain MRI separation study indicated good precision, as well as the area of technology, had great reliability in the anatomical outcomes of the classification of brain MRI. The MRI characteristics of CI patients were retrieved using a convolutional network, and the results were outstanding. Since the network has not saved the segmented image and processed it, hence the features are not clearly estimated.

Brain tumours were classified using DL characteristics and machine learning algorithms by the authors in [13]. The support vector machine (SVM) with the basis function kernel outperformed other machine learning classifiers, and the incorporation of DL greatly enhanced effectiveness. Additionally, the properties of the sensors were examined, and the WHGO descriptor demonstrated outstanding recognition accuracy for the model classifiers. But it is also time-consuming and operator-dependent.

In [14] the objective of this study is to create a screening method to identify hydrocephalus cases from head MRIs. A 3D convolutional neural network was utilised to autonomously partition the other 480 exams and retrieve volumetric anatomical information after being trained on 16 manual segmentation exams (ten of which had hydrocephalus). On 240 exams, a logistic learner of these variables was developed to spot instances of hydrocephalus that needed surgical treatment for therapy. This approach can speed up and improve neuroradiology reads as well as help with the diagnosis of probable hydrocephalus. Still, this method needs to be further enhanced to be automated.

The fuzzy brain-storm optimal solution, which combines fuzzy and brain-storm objective functions, was suggested by the authors in [15] for the segmentation and classification of medical images. Brainstorm optimizing

prioritises the cluster centroids and focuses on them; like other swarm techniques, it may fall into local optimization. The brain-storm optimizer is interesting and surpasses the other strategies with superior outcomes in this investigation. The fuzzy runs numerous cycles to propose an ideal network model. But it can only be used to detect high-grade hydrocephalus.

Study [10] still needs to rely on data. In [11] there is a need to enhance the accuracy of the paper by utilizing the data from the features in an efficient manner. In [12], the network has not saved the segmented image and processed it, hence the features are not clearly estimated. Paper [13] is time-consuming and operator-dependent, [14] must be further enhanced to be automated and [15] can only be used to detect high-grade hydrocephalus. So, there is a need to develop a model which can overcome all the above-mentioned issues in an accurate manner.

3. H-Detect Framework for Prediction of Hydrocephalus. This research work proposes a code-based H-detect model that pre-processes MRI brain images, segments them using Fuzzy and extracts the necessary features, based on the features classifies them, and predicts them for early recognition of hydrocephalus. We used an original dataset of 100 patients from several testing facilities to test the algorithm. In order to extract better features and weed out incorrect predictions, the input photos are first pre-processed to reduce noise and normalise the image into a similar comprehensible format. Then the normalized images are segmented using the triangular membership function in fuzzy rules for Edge detection. The edge-featured images are then used as a training and testing set. For training and testing, we use datasets from the UCI machine learning laboratory and mridata.org for our larger requirements. The training and testing set includes characteristics of healthy individuals and cancer patients at various stages. CatBoost is an open-source platform that is tailored in this paper to predict hydrocephalus. CatBoost is an excellent choice because of its resilience, capacity to handle various datasets from various sources, work on non-numeric data and lack of knowledge of rigorous data preparation. The algorithm can also accept categorical variables without displaying the conversion type mistake, allowing the programmer to fine-tune the model rather than correcting trivial errors.

The H-detect framework is a combination of segmentation techniques, triangular fuzzy rules and the CatBoost algorithm. Feature extraction is done by segmenting the image based on edge detection using triangular fuzzy rules. Therefore, the exact information on the structure of CSF inside the brain is efficiently highlighted. The segmented images are given to the CatBoost algorithm. Thus, the H-detect strategy efficiently predicts hydrocephalus.

Steps followed in the proposed method:

Step 1. Pre-process image to remove noise.

Step 2. Design fuzzy input and outputs.

Step 3. Define membership functions.

Step 4. Define Fuzzy rules.

Step 5. Fuzzified images to get the segmented images.

Step 6. Label the segmented images and add them to the digitized dataset.

Step 7. Construct a structure and append labels and images to that.

Step 8. Split the data into training and testing sets.

Step 9. Apply the CatBoost algorithm to generate results.

Step 10. Take an MRI of a new patient and segment using fuzzy rules in step 2. Create labelled data.

Step 11. Apply predictive analysis.

The proposed method, H-detect, can be categorized into three sections: pre-processing, segmentation, and classification as shown in Figure 1. The subsequent sub-sections explain the overall methodology under the three steps mentioned earlier.

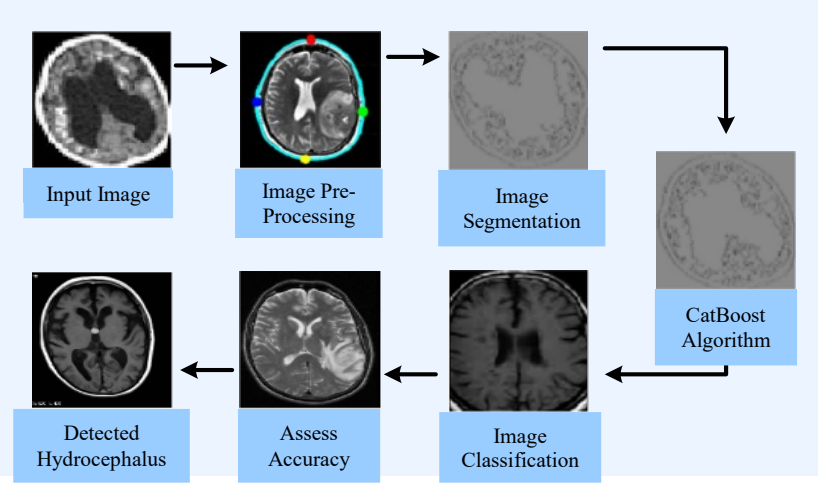

Fig. 1. Process flow diagram of the proposed H-detect method

3.1. Pre-processing. In computer-aided medical diagnostics, image pre-processing is a crucial component, specifically in hydrocephalus-related classification, thereby the segmentation and feature extraction algorithms can perform efficiently. Accurate hydrocephalus detection and segmentation lead to precise feature extraction and classification of

hydrocephalus. If the image is pre-processed according to image size and quality, precise hydrocephalus segmentation is feasible which is essential since most real-world data is noisy, inconsistent, and incomplete.

The quality of the acquisition equipment to capture the scene being imaged, such as the structures of the human body, is fundamental for visual interpretation and analysis of digital pictures. It is standard procedure to pre-process images to adjust or improve them before feeding them into more sophisticated processing steps. When deep machine learning is used to edit images, common pre-processing tasks include adjusting their initial dimensions and the augmentation of their intensity. Before feeding the learning machines, the dimensions of the input images are normally reduced to an appropriate size. The basic assumption of size reduction is to reduce the learning machines' compute times at the rate of image quality.

There is a requirement to establish a baseline dimension for all photos input into our AI algorithms in order to extract the features quickly without generating any incorrect predictions because the size of some images captured by the camera and provided to our AI technology fluctuates. The proposed framework employs the following approach to eliminate noise and provide a suitable scale to the input image shown in Figure 2.

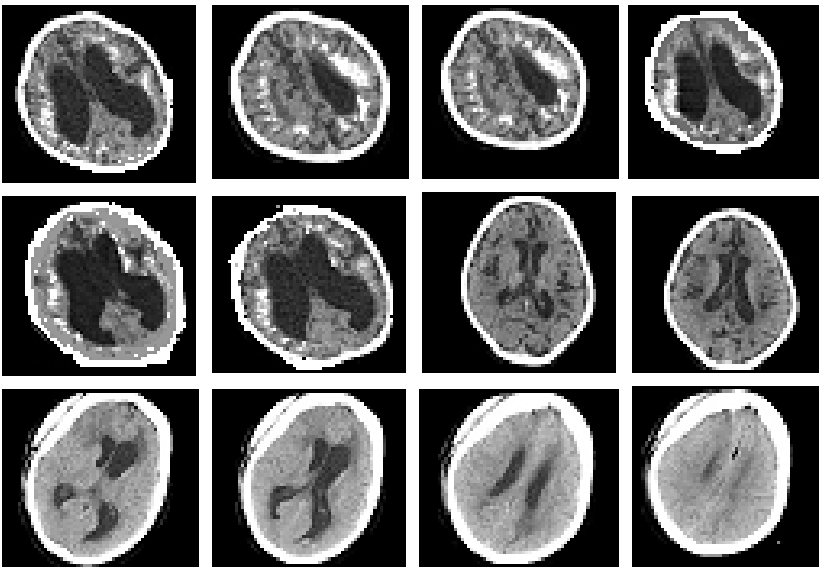

Fig. 2. MRI Image of the brain with Hydrocephalus

Algorithm 1. Pre-processing

Setup: Initialize required variables
Start
Step 1: Read the MRI image
Step 2: Get the dimensions of the image I
Step 3: Get a grey threshold of Ig
Step 4: Get the class type of red channel of I
Step 5: Determine the scaling factor
Step 6: Get a red channel of I
Step 7: I_{scaled} = Ig/scaling Factor

In this paper, the input image is first imparted to the H-Detect algorithm, which retrieves the image information first. Sound interruption, offset field effects, and short-channel impacts could happen while processing brain images. The converted grey threshold function is then used to compute a threshold value. As just one channel is evaluated in each iteration, the algorithm determines the original image's grey threshold value. The image's scaling factor is also determined using the threshold value and Class type.

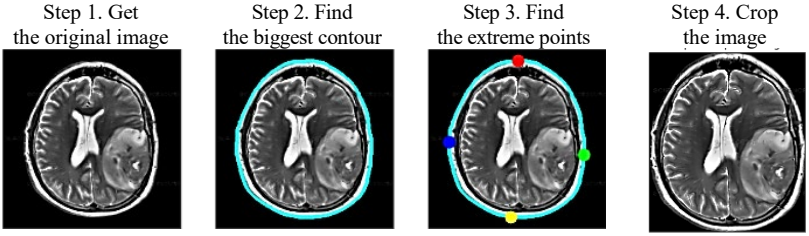

Fig. 3. Pre-processing steps involved in the proposed method

Figure 3 clearly shows the normalization of the image by finding the biggest contour, finding the extreme points and scaling the image. Finally, one image channel is retrieved and split by the scaling factor to generate a normalized image, allowing the algorithm to gather features through correct segmentation and eliminating erroneous classification. The next phase in identifying Hydrocephalus is feature extraction with segmentation, detailed in the next section.

3.2. Segmentation based feature extraction. The process of simplifying and modifying the representation of an image into a much more relevant and simpler form to analyse is known as segmentation. Image segmentation is commonly used to find objects and borders in images. Medical image segmentation is critical in demarcating areas of interest

under investigation. It is required in nearly all medical imaging applications and is necessary for automated disease state identification in diagnostic imaging. Nevertheless, because of separate variations and the difficulty of human organs like the brain, segmentation outputs from medical images, particularly those of brain hydrocephalus, are insufficient.

Medical brain pictures are ambiguous by nature and are therefore rife with ambiguity in diagnosis and prediction. The pixel grayscale border between the limit of the brain image and the background becomes hazy and overlapped due to the interaction between light and spatial resolution with brain pictures. It is also challenging to accurately depict the connections between the borders, points, and areas of the locations in the scene due to the influence of equipment elements, which increases the uncertainty, since voxels on a boundary often include two substances, such as border and item.

In order to improve the effectiveness of brain image classification as well as diagnostics, this work makes use of the boundary information of unlabelled and labelled data in brain medical imaging. The human brain MRI image is divided into various situations. Finally, the enhanced algorithm creates a brain disorder medical image segmentation system via fuzzy rules with a triangular membership function.

Algorithm 2. Segmentation

Setup: Initialize required variables from the pre-processed image

Start

Step 1: Create a new fuzzy structure based on the triangular membership function.

$$f(x) = \mathrm{m} \quad \left(\mathrm{m} \quad \left(\frac{x-a}{b-a}, \frac{c-x}{c-b}\right), 0\right), \tag{1}$$

where $f(x)$ is the Triangular membership function,

a, b, c are the parameters,

x is the input value.

Step 2: Add image gradients as input and add output variables.

Step 3: Declare the membership function as $P_{1_{2in}}, P_i$.

$$\mu(F_s) = \begin{cases} 0 \text{ if Fs} \le w \\ \dfrac{(F_s - w)}{(b - w)} \text{ if w} \le F_s \le \text{b} \\ \dfrac{(e - Fs)}{(e - b)} \text{ if b} \le F_s \le \text{e} \\ 0 \text{ if Fs} \ge \text{e} \end{cases}, \quad (2)$$

where $\mu(F_s)$ is the membership function,

Fs is universe of discourse,

w is white,

b is black,

e is edge.

Step 4: If all the membership function equals 0, then black.

Step 5: If anyone or more numbers of the membership function are not equal to 0, then edge.

Step 6: If all the membership functions are not equal to 0, then white.

Step 7: Create an empty matrix for the output.

Step 8: Collect the rules, and create the array.

Step 9: Evaluate fuzzy rules and add the rules to FIS based on the following function:

$$\sum_{\forall R} \sum_{\forall G} \sum_{\forall B} F(I_{mri})_{\forall RGB}, \quad (3)$$

where $\forall R$: Red Channel,

$\forall G$: Green Channel,

$\forall B$: Blue Channel,

I_{mis}: Pre-processed MRI image, (dcom converted to jpg).

Step 10: Segment the image based on fuzzy rule-based feature extracted image:

$$\sum_{\nabla_{\text{mi}}} \text{I}_{\text{mri}} \cap \text{F}(\text{I}_{\text{mri}}), \quad (4)$$

where $\forall_{mri}$: All the elements of the MRI image,

S_{seg}: Edges detected using (3),

I_{mri}: Pre-processed MRI image (converted into jpg),

$F(I_{mri})$: Fuzzified image.

The segmentation is computed with fuzzy membership values using the triangular membership function. The augmented image shown in Figure 4 obtained after pre-processing for separate channels is taken as input. Then the proposed H-detect has designed a fuzzy model to segment

the RGB MRI images with a triangular membership function. The mathematical representation of the triangular membership function is explained in steps 1 and 3. The images are segmented with different membership functions to choose the right membership function as shown in Figure 5. The other parameters remained the same. The functions in steps 9 and 10 are employed to design the Fuzzy model, and then the designed rules are applied to detect the edges. The whole algorithm is repeated for green and blue channels also. Thus finally, the segmented RGB image is obtained by overlaying the segmented R, B and G channel images.

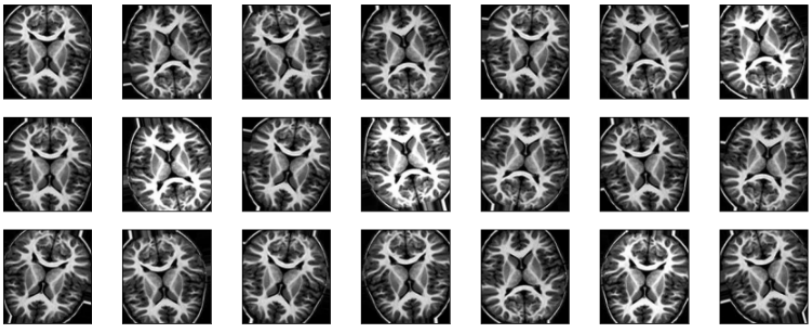

Fig. 4. Augmented image with a single channel for edge detection

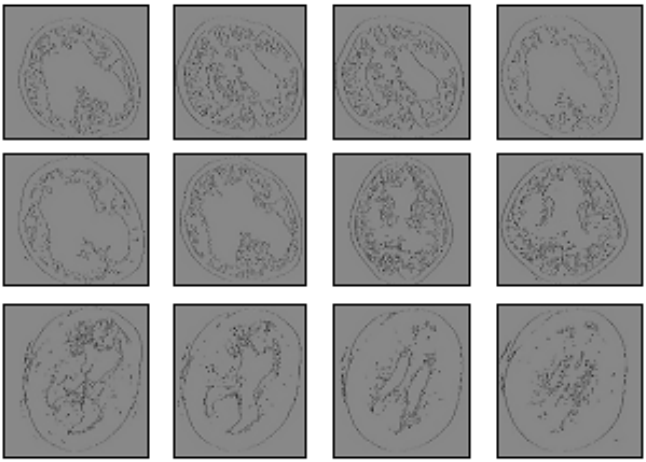

Fig. 5. Segmented Hydrocephalus Images

3.3. Classification. All the segmented images are stored in a folder and are scaled to bring uniformity. The scaled images are read one by one

from the folder, and a threshold value is predicted by calculating the mean of the minima of an Image. The threshold of all the images is summed up and then divided by the number of images in the folder. It gives us the scaling factor. The folder is again iterated, and every image is divided by the scaling factor and forms the image dataset; thus, the image will be free from all falsifying factors, enhancing accuracy.

Then a label is assigned to each dataset for classification. Before applying CatBoost, the data type is changed to float. It is then flattened and then divided by 255 (pixel value). We use steps 4 and 5 to design the model and then fit the data on the model. Once the model fits, a new image is taken, and predictive analysis is done, as explained in Step 7.

Setup: Initialize required variables

Start

Step 1. Read folder having Edge featured images.

Step 2. Create a learning dataset using fn (3):

$$\sum_{i=1}^{\nabla S_{eg}} \left\{F\left(S_{seg}\right)_i\right\}, \tag{5}$$

where $\forall S_{seg}$: All the elements of the segmented image from (4)

$\left\{F\left(S_{seg}\right)_i\right\}$: The segmented image taken as features

Step 3. Label the data.

Step 4. Create the CatBoost classifier model:

$$\sum_{i=1}^{\nabla S_{\text{see}}} \left\{F\left(S_{seg}\right)_i\right\}, \tag{6}$$

where $\forall S_{seg}$: All the elements of the segmented image from (4),

$\left\{F\left(S_{seg}\right)_i\right\}$: The segmented image taken as features.

Step 5. Train the CatBoost classifier model with training data:

$$\sum_{\nabla F} D_c(\{F_{\text{train}}, \mathrm{F}_{\text{test}}\}), \tag{7}$$

where $\forall F$: All the features,

$D_c\left(\left\{F_{\text{train}}, F_{\text{test}}\right\}\right)$: Apply CatBoost on the Training and testing set Created after (6).

Step 6. Fit the model on Dataset, Data Label.

Step 7. Test the model using (8):

$$\sum_{\nabla R} \mathrm{P}(\forall \mathrm{R}, \mathrm{N}_{\text{feature}}), \tag{8}$$

where $\forall R$: Results of CatBoost,

$\mathrm{P}(\forall \mathrm{R}, \mathrm{N}_{\text{feanive}})$: Predictive analysis of New Features.

The CatBoost classifier is one machine learning technique that's also effective in forecasting classified variables. Gradient boosting is carried out via CatBoost, which uses binary decision trees as baseline forecasts [16]. Suppose we observe data with samples $D = \{(X_j, y_j)\}_{j=1,\dots,m}$, where $x_j = x_j^1, x_j^2, \dots\dots\dots, x_j^n$ vector of n features and response feature $y_j \in R$, which can be binary (i.e., yes or no) or encoded as a numerical feature (0 or 1). Samples (X_j, y_j) are independently and identically distributed according to some unknown distribution $(\cdot,\cdot)$. The goal of the learning task is to train a function $H : R^n \rightarrow R$, which minimizes the expected loss given as:

$$\mathcal{L}(H) = EL\big(y, H(X)\big), \tag{9}$$

where $L(\cdot,\cdot)$ is a smooth loss function, and (X, y) is testing data sampled from the training data D.

The procedure for gradient boosting constructs iteratively a sequence of approximations $H^t: R^m \rightarrow R, t = 0, 1, \dots$ in a greedy fashion. From the previous approximation H^{t-1}, H^t is obtained in an additive process, such that $H^t = H^{t-1} + \alpha g^t$. With a step size α and function $g^t : R^n \rightarrow R$, which is a base predictor, is selected from a set of functions G to reduce or minimize the expected loss defined below:

$$g^t = \arg min_{g \in G} \mathcal{L}(H^{t-1} + g), \tag{10}$$

$$= \arg min_{g \in G} EL\big(y, H^{t-1}(X) + g(X)\big). \tag{11}$$

Often, the minimization problem is approached by the Newton method using a second-order approximation of $L(H^{t-1} + g^t)\ at H^{t-1}$ or by taking a (negative) gradient step.

Thus, the suggested H-detect algorithms accurately identify Hydrocephalus in brain MRI images with minimal processing time. One of the predictions is depicted in Figure 6. The suggested technique effectively eliminates incorrect predictions and overfitting. The next part evaluates and discusses the results gained by applying the proposed strategy and its performance.

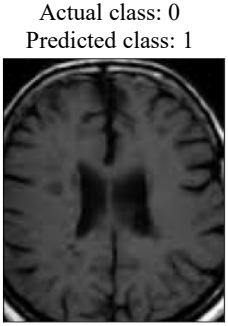

Fig. 6. Prediction of labelled image classes

4. Result and Discussion. The proposed H-detect technique is implemented in MATLAB. MRI images are converted from DCOM to jpg format using a third-party tool. If we discuss about pattern recognition we may use the YOLO technique but in this section, we initialized the basic approach to segmentation for hydrocephalus detection. 3D image processing technique is used for visualization, processing, and analysis of 3D image data through geometric transformations. The 3D approach can be also applicable for such tasks since CT is a sequence of images of a brain and the 3D approach can also be useful for the diagnosis of hydrocephalus with a couple of datasets. 3D is an older technique. Here, we use the Catboost algorithm which is used for prediction and classification. It is much better than 3D for various factors such as segmentation, classification, decision-making, precision and accuracy. By applying Catboost with fuzzy logic, the proposed system works better than the existing work. The output of the implementation and the obtained results are discussed in this section.

4.1. System Configuration.

Processor : Intel Core i5, V generation
RAM : 16 GB
Graphics : Nvidia
HDD : 1 TB
OS : Windows 10

4.2. Dataset description. Hydrocephalus datasets from three testing labs have been taken. Due to the non-disclosure agreement, further details cannot be shared. The dataset also includes records of Tumor, Malignant, Benign, and Hydrocephalus which were taken from Brigham and Women's Hospital, Surgical Planning Laboratory, Department of Radiology, Harvard Medical School (Boston, MA, USA), BRATS, BITE, metadata.org, and cancerimagingarchive.net.

4.3. Implementation results. The image of Figure 7, 8 shows the input dataset containing both brain MRI images with and without hydrocephalus. The distribution of the images with respective ratio values is given below in Figure 9. The H-detect model predicts the hydrocephalus efficiently.

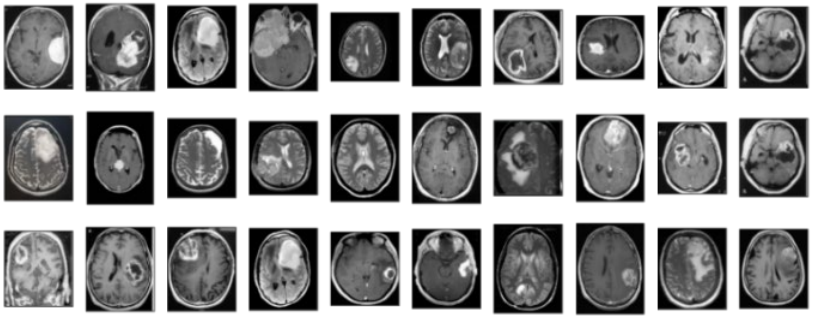

Fig. 7. Dataset images with hydrocephalus

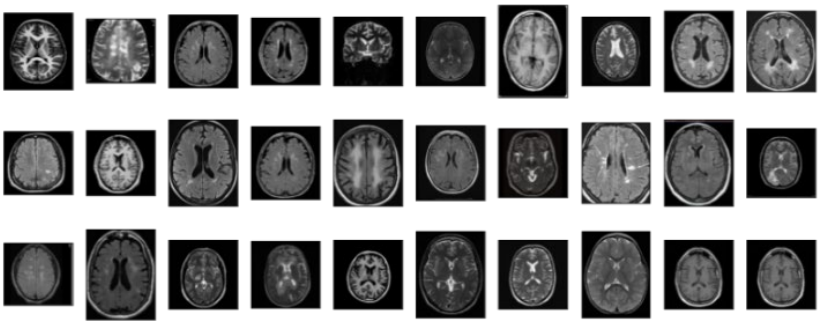

Fig. 8. Dataset images without hydrocephalus

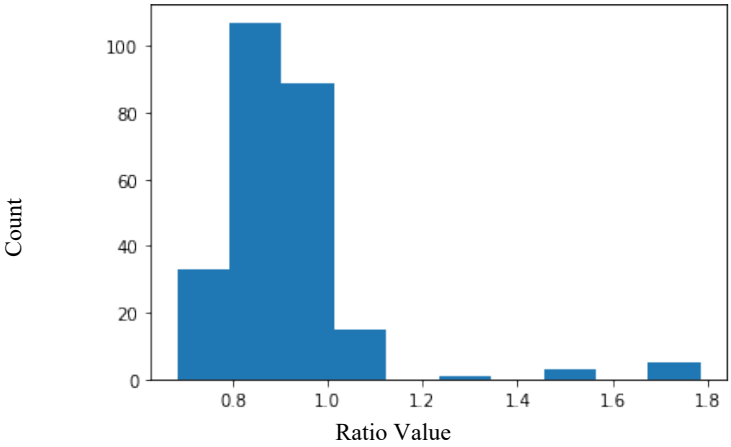

Fig. 9. Distribution of Image Ratios

The cat boost model has 34 Iterations, 0.05 Learning rate, depth of 12 and multi-class loss function.

4.4. Performance metrics. The following formulae from (12) to (15) are calculated for checking the robustness of H-detect Precision, Recall, Accuracy, and F1 scores. True Positive (TP), True Negative (TN), False Positive (FP), and False Negative (FN) are the metrics used to calculate the scores:

$$Precision = \frac{TP}{(TP + FN)}, \tag{12}$$

$$Recall = \frac{TN}{(TN + FP)}, \tag{13}$$

$$Accuracy = \frac{(TP + TN)}{(TP + TN + FP + FN)}, \tag{14}$$

$$F1 = \frac{2 \times (Precision \times Recall)}{(Precision + Recall)}. \tag{15}$$

The confusion matrix that was produced after using the proposed approach is shown in Figure 10. A True Positive (TP) value of 19, a True Negative (TN) value of 0, a False Positive (FP) value of 1, and a False

Negative (FN) value of 30 are displayed in the matrix. Thus, utilizing the proper extracted features obtained from the fuzzy triangular membership function increases the accuracy which is clear as the model has just a 1% loss.

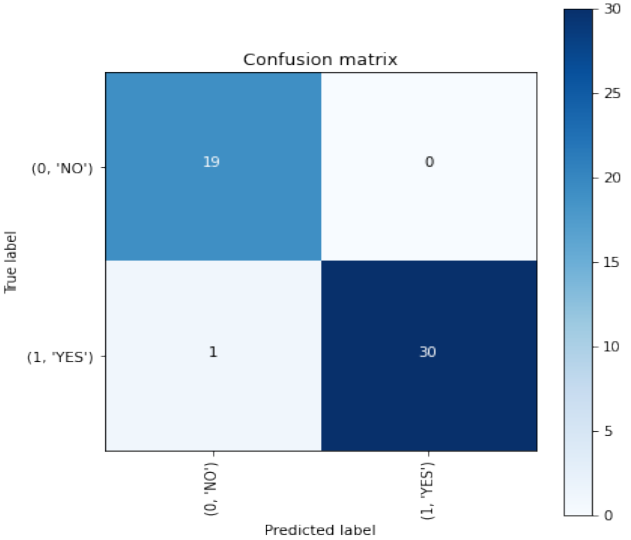

Fig. 10. Confusion matrix obtained for the proposed method

The proposed model's accuracy and loss function are depicted above in Figure 11. The validation set performs significantly better than the training set as the CatBoost algorithm performs efficient prediction. With 40 epochs, the maximum accuracy of 0.99 was achieved. The validation set's loss is similarly lower than the training sets. With 40 epochs, only 0.1 of loss was observed.

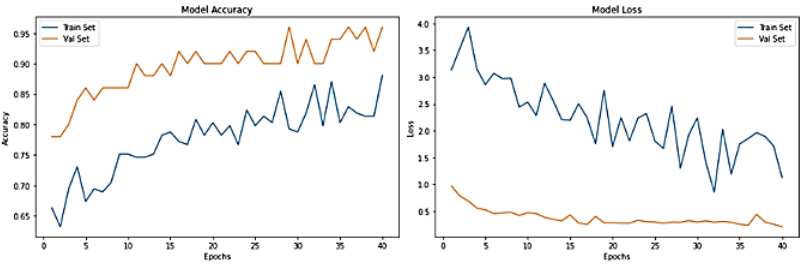

Fig. 11. Performance Graph obtained for the proposed method

Table 1 displays the performance of the proposed H-detect method based on its precision, accuracy, F1 score and recall. As this research removed the unwanted noises, normalized and extracted features from fuzzy logic and utilized the CatBoost algorithm for prediction the findings indicate that the proposed technique has obtained 99% precision, accuracy, F1 score, and 100% recall.

Table 1. Performance metrics of the proposed method

Performance measures	Value
Precision	0.99009901
Recall	1
Accuracy	0.995
F1-score	0.995025

4.5. Comparison Metrics. Table 2 shows the variation in time taken for the segmentation proposed method compared with Consecutive deep encoder-decoder networks, Morphological adaptive fuzzy thresholding and Fuzzy c-means. The graph shows that a Consecutive deep encoder-decoder network takes 3021 ms, Morphological adaptive fuzzy thresholding takes 1894 ms, and Fuzzy c-means takes 189 ms. Our proposed method, H-detect, takes just 62 ms, as fuzzy logic uses the triangular membership function which is much faster than the conventional methods.

Table 2. Comparison of time taken in segmentation with different techniques

Model	Time (in ms)
[17] Consecutive Deep Encoder-Decoder Network	3021
[18] fuzzy c-means	189
[19] Morphological Adaptive Fuzzy Thresholding	1894
H-detect	62

Table 3 above exhibits how the proposed methodology compares to the Consecutive deep encoder-decoder network, Morphological adaptive fuzzy thresholding, and Fuzzy c-means in terms of classification duration. The graph shows that the Deep Convolutional Neural Network requires 261 milliseconds, Spark-based parallel fuzzy c-means requires 278 milliseconds, F score-based method requires 176 milliseconds. Our proposed method, H-detect requires only 98 milliseconds, which is significantly superior to the conventional methods by utilization of the CatBoost algorithm.

Table 3. Comparison of time taken in classification with different techniques

Model	Time (in ms)
[20] Deep Convolutional Neural Network	261
[18] Spark-based parallel fuzzy c-means	278
[21] F score-based method	176
H-detect	98

Table 4 tends to parallel the accuracy of the proposed method founded on the membership function used. The proposed method uses triangular membership, compared with singleton, gaussian, generalized bell, and sigmoidal functions. The results show that the proposed membership function has 100% exactness, accurateness, F1 score and recall, which shows that the proposed triangular membership function is the most superior function to the traditional one in all aspects.

Table 4. Performance metrics based on membership function

Membership Functions	Precision	Accuracy	F1-score	Recall
Singleton	0.900901	0.945	0.947867	1
Gaussian	0.925926	0.96	0.961538	1
Generalized Bell	0.884956	0.935	0.938967	1
Sigmoidal	0.943396	0.97	0.970874	1
Trapezoidal	0.961538	0.98	0.980392	1
Triangular	1	1	1	1

Table 5 compares the suggested method's performance dependent on various types of cancer data like tumour, benign, malignant and Hydrocephalus. The suggested technique compares the exactness, correctness, F1 score and recall. The findings indicate that 100 percent exactness, accurateness, F1 score, and recall have been obtained for Hydrocephalus, demonstrating that the proposed H-detect method is outstanding to the conventional one.

Table 5. Performance based on the type of cancer

Type	Precision	Accuracy	F1-score	Recall
Tumour	0.99009901	0.995	0.9950249	1
Benign	0.981	0.99	0.989	1
Malignant	0.980392157	0.99	0.990099	1
Hydrocephalus	1	1	1	1

Table 6 shows the accuracy of 7 various methods compared with our proposed method with and without noise. The graphs depict that the proposed method has shown outstanding results than the previously proposed method, with 99.9% accuracy with and without noise as the pre-processing step efficiently contributes to the accuracy.

Table 6. Accuracy comparison with different techniques

Method	With Noise	Without Noise
[22] KM	0.9720	0.6239
[23] RKM	0.9743	0.7832
[24] FCM	0.9728	0.7698
[25] RFCM	0.9782	0.7806
[26] GRFCM	0.9679	0.7622
[27] SFRCM	0.9264	0.7786
[28] RIFCM	0.8992	0.9016
Proposed	0.99	0.99

Table 7 compares three other conventional models based on precision, accuracy, F1 score and recall. The results obtained showed that the proposed model has the best precision of 99%, the accuracy of 99.5%, the F1 score of 99.5 %, and the recall of 100% proving that the proposed method is the best one with précised pre-processing step, fuzzy logic with triangular membership function-based segmentation, edge-based features and the CatBoost classification methodology.

Table 7. Comparison of performance with different techniques

Algorithm	Precision	Accuracy	F1-score	Recall
[29] Fuzzy Reasoning Model	0.917431193	0.955	0.956938	1
[30] Modified Timed Automata Model	0.934579439	0.965	0.966184	1
[31] Gaussian Mixture Model	0.952380952	0.975	0.97561	1
H-Detect	0.99009901	0.995	0.995025	1

5. Conclusion. This research adopted MRI data to detect various kinds of Hydrocephalus early. The brain and hydrocephalus volumes are heavily influenced by the spatial resolution of successive brain cross-sections and the slice thickness employed during CT imaging. As a result, the focus of this study is on two major enhancements. Firstly, the image segmentation method will be enhanced, allowing for better separation of the targeted brain areas by utilizing a neural fuzzy method with a triangular

membership function. Then for predictive analysis, a classifier based on the cat boost method is presented to classify Hydrocephalus. For novelty, we aggregate the fuzzy rules and CatBoost for better results. According to the observations, the suggested model has a precision, accuracy, and an F1 score of 99% and a recall of 100%. In each aspect, the comparative findings have shown to be superior to the conventional ones. As a result, the proposed H-detect approach can reliably diagnose Hydrocephalus early without any false predictions or overfitting issues, allowing numerous people's lives to be saved. In future studies, we may impose a particular feedback system to monitor the diagnosis system for hydrocephalus in a medical era so that the processing time may be reduced.

References

1. Zhang X.J., Guo J., Yang J. Cerebrospinal fluid biomarkers in idiopathic normal pressure hydrocephalus. Neuroimmunology and Neuroinflammation. 2020. vol. 7. no. 2. pp. 109–119.
2. Karimy J.K., Reeves B.C., Damisah E., Duy P.Q., Antwi P., David W., Kahle K.T. Inflammation in acquired Hydrocephalus: pathogenic mechanisms and therapeutic targets. Nature Reviews Neurology. 2020. vol. 16. no. 5. pp. 285–296.
3. Paulsen A.H. Adult outcome in pediatric Hydrocephalus. 2018. 58 p.
4. Saygili G., Yigin B.O., Guney G., Algin O. Exploiting lamina terminalis appearance and motion in the prediction of Hydrocephalus using convolutional LSTM network. Journal of Neuroradiology. 2022. vol. 49. no. 5. pp. 364–369.
5. Nakajima M., Kawamura K., Akiba C., Sakamoto K., Xu H., Kamohara C., Miyajima M. Differentiating comorbidities and predicting prognosis in idiopathic normal pressure hydrocephalus using cerebrospinal fluid biomarkers. Croatian Medical Journal. 2021. vol. 62. no. 4. pp. 387–398.
6. Yigin B.O., Algin O., Saygili G. Comparison of morphometric parameters in prediction of Hydrocephalus using random forests. Computers in Biology and Medicine. 2020. vol. 116. no. 103547.
7. Chiarelli P.A., Hauptman J.S., Browd S.R. Machine learning and the prediction of Hydrocephalus: Can quantitative image analysis assist the clinician? JAMA paediatric. 2018. vol. 172. no. 2. pp. 116–118.
8. Chen J., He W., Zhang X., Lv M., Zhou X., Yang X., Xia J. Value of MRI-based semi-quantitative structural neuroimaging in predicting the prognosis of patients with idiopathic normal pressure hydrocephalus after shunt surgery. European Radiology. 2022. vol. 32. no. 11. pp. 7800–7810.
9. Sotoudeh H., Sadaatpour Z., Rezaei A., Shafaat O., Sotoudeh E., Tabatabaie M., Tanwar M. The Role of Machine Learning and Radiomics for Treatment Response Prediction in Idiopathic Normal Pressure Hydrocephalus. Cureus. 2021. vol. 13. no. 10.
10. Mao Y., Shen Z., Wang J., Zhu H., Yu Z., Chen X., Cheng H. Deep Learning-Based MR Imaging for Analysis of Relation between Cerebrospinal Fluid Variation and Communicating Hydrocephalus after Decompressive Craniectomy for Craniocerebral Injury. Scientific Programming. 2022. vol. 2022.
11. Brito C., Machado A., Sousa A.L. Electrocardiogram beat classification based on a Res-Net network. Studies in Health Technology and Informatics. 2019. vol. 264. pp. 55–59.

12. Hu Y., Zhao H., Li W., Li J. Semantic image segmentation of brain MRI with deep learning. Zhong nan da XueXueBao. Yi Xue ban Journal of Central South University. Medical sciences. 2021. vol. 46. no. 8. pp. 858–864.
13. Kang J., Ullah Z., Gwak J. MRI-based brain tumour classification using ensemble of deep features and machine learning classifiers. Sensors. 2021. vol. 21(6). no. 2222.
14. Huang Y., Moreno R., Malani R., Meng A., Swinburne N., Holodny A.I., Young R.J. Deep Learning Achieves Neuroradiologist-Level Performance in Detecting Hydrocephalus Requiring Treatment. Journal of Digital Imaging. 2022. vol. 35. no. 6. pp. 1662–1672.
15. Narmatha C., Eljack S.M., Tuka A.A.R.M., Manimurugan S., Mustafa M. A hybrid fuzzy brain-storm optimization algorithm for the classification of brain tumour MRI images. Journal of ambient intelligence and humanized computing. 2020. pp. 1–9.
16. Prokhorenkova L., Gusev G., Vorobev A., Dorogush A.V, Gulin A. CatBoost: Unbiased Boosting with Categorical Features. Advances in Neural Information Processing Systems. 2018. vol. 31. pp. 6638–6648.
17. Nguyen N.Q., Lee S.W. Robust Boundary Segmentation in Medical Images Using a Consecutive Deep Encoder-Decoder Network. IEEE Access. 2019. vol. 7. pp. 33795–33808. DOI: 10.1109/ACCESS.2019.2904094.
18. Liu B., He S., He D., Zhang Y., Guizani M. A Spark-based Parallel Fuzzy c-Means Segmentation Algorithm for Agricultural Image Big Data. IEEE Access. 2019. vol. 7. pp. 42169–42180. DOI: 10.1109/ACCESS.2019.2907573.
19. Almotiri J., Elleithy K., Elleithy A. A Multi-Anatomical Retinal Structure Segmentation System for Automatic Eye Screening Using Morphological Adaptive Fuzzy Thresholding. IEEE Journal of Translational Engineering in Health and Medicine. 2018. vol. 6. pp. 1–23. DOI: 10.1109/JTEHM.2018.2835315.
20. Liu M., Jiang J., Wang Z. Colonic Polyp Detection in Endoscopic Videos with Single Shot Detection Based Deep Convolutional Neural Network. IEEE Access. 2019. vol. 7. pp. 75058–75066. DOI: 10.1109/ACCESS.2019.2921027.
21. Raweh A.A., Nassef M., Badr A. A Hybridized Feature Selection and Extraction Approach for Enhancing Cancer Prediction Based on DNA Methylation. IEEE Access. 2018. vol. 6. pp. 15212–15223. DOI: 10.1109/ACCESS.2018.2812734.
22. Gonzalez R., Tou J. Pattern recognition principles. Applied Mathematics and Computation. Reading, MA: Addison-Wesley. 1974. 377 p.
23. Lingras P., West C. Interval set clustering of web users with rough k-means. Journal of Intelligent Information Systems. 2004. vol. 23. no. 1. pp. 5–16. DOI: 10.1023/B:JIIS.0000029668.88665.1a.
24. Chuang K.S., Tzeng H.L., Chen S., Wu J., Chen T.J. Fuzzy c-means clustering with spatial information for image segmentation. Comput. Med. Imag. Graph., Jan. 2006. vol. 30. no. 1. pp. 9–15. DOI: 10.1016/j.compmedimag.2005.10.001.
25. Lingras P., Peters G. Applying rough set concepts to clustering. In Rough Sets: Selected Methods and Applications in Management and Engineering. London: Springer. 2012. pp. 23–37.
26. Ji Z., Sun Q., Xia Y., Chen Q., Xia D., Feng D. Generalized rough fuzzy c-means algorithm for brain MR image segmentation. Computer methods and programs in biomedicine. 2012. vol. 108. no. 2. pp. 644–655.
27. Namburu A., Srinivas Kumar S., Srinivasa Reddy E. Review of Set-Theoretic Approaches to Magnetic Resonance Brain Image Segmentation. IETE Journal of Research. 2022. vol. 68. no. 1. pp. 350–367. DOI: 10.1080/03772063.2019.1604176.
28. Dubey Y.K., Mushrif M.M., Mitra K. Segmentation of brain MR images using rough set based intuitionistic fuzzy clustering. Biocybern. Biomedical engineering. 2016. vol. 36. no. 2. pp. 413–426. DOI: 10.1016/j.bbe.2016.01.001.

29. Liu J., Peng Y., Zhang Y.A Fuzzy Reasoning Model for Cervical Intraepithelial Neoplasia Classification Using Temporal Grayscale Change and Textures of Cervical Images during Acetic Acid Tests. IEEE Access. 2019. vol. 7. pp. 13536–13545. DOI: 10.1109/ACCESS.2019.2893357.
30. Brunese L., Mercaldo F., Reginelli A., Santone A. Prostate Gleason Score Detection and Cancer Treatment through Real-Time Formal Verification. IEEE Access. 2019. vol. 7. pp. 186236–186246. DOI: 10.1109/ACCESS.2019.2961754.
31. Yin S., Zhang Y., Karim S. Large Scale Remote Sensing Image Segmentation Based on Fuzzy Region Competition and Gaussian Mixture Model. IEEE Access. 2018. vol. 6. pp. 26069–26080. DOI: 10.1109/ACCESS.2018.2834960.

Baloni Dev — Ph.D., Dr.Sci., Associate professor, Quantum school of technology, Quantum University. Research interests: image processing, machine learning, deep learning, artificial intelligence. The number of publications — 20. devbaloni1982@gmail.com; Dehradun Highway, Mandawar, 247167, Roorkee, Uttarakhand, India; office phone: +91(8755)507-830.

Rai Dhajvir Singh — Assistant professor, School of engineering and computing, Dev Bhoomi Uttarakhand University. Research interests: cloud computing, machine learning, deep learning, artificial intelligence. dhajvirrai123@gamil.com; Chakrata Road, Manduwala, 248007, Naugaon, Uttarakhand, India; office phone: +91(9557)891-499.

Sivagaminathan PG — Professor, School of engineering, Ajeenkya D.Y Patil University. Research interests: information retrieval, pattern recognition, AI, machine learning, deep learning. The number of publications — 31. sai.sivagaminathan@gmail.com; City Road via Lohegaon, 412105, Charholi Budruk, Pune, Maharashtra, India; office phone: +91(9500)903-614.

Anandaram Harishchander — Ph.D., Dr.Sci., Assistant professor, Amrita school of artificial intelligence, Amrita Vishwa Vidyapeetham (Amrita University). Research interests: computational systems biology, functional genomics, developmental biology. The number of publications — 43. a_harishchander@cb.amrita.edu; Amritanagar, Ettimadai Village, 641112, Coimbatore, Tamil Nadu, India; office phone: +91(9940)066-227.

Thapliyal Madhur — Assistant professor, Graphic Era Hill University. Research interests: cyber security, image processing, deep learning, machine learning. The number of publications — 3. madhurthapliyal@gehu.ac.in; Bell Road, Clement Town, 248002, Dehradun, Uttarakhand, India; office phone: +91(7017)747-897.

Joshi Kapil — Ph.D., Dr.Sci., Assistant professor, Uttaranchal institute of technology, Uttaranchal University. Research interests: image fusion, image processing, deep learning, CNN. The number of publications — 132. Kapilengg0509@gmail.com; Prem Nagar, 248007, Dehradun, Uttarakhand, Russia; office phone: +91(8979)799-289.

DOI 10.15622/ia.23.2.7

Д. БАЛОНИ, Д. РАЙ, П. СИВАГАМИНАТАН, Х. АНАНДАРАМ, М. ТАПЛИЯЛ, К. ДЖОШИ

H-DETECT: АЛГОРИТМ РАННЕГО ВЫЯВЛЕНИЯ ГИДРОЦЕФАЛИИ

Балони Д., Рай Д., Сивагаминатан П., Анандарам Х., Таплиял М., Джоши К. **H-Detect: алгоритм раннего выявления гидроцефалии.**

Аннотация. Гидроцефалия – это заболевание центральной нервной системы, которое чаще всего поражает младенцев и детей ясельного возраста. Оно начинается с аномального накопления спинномозговой жидкости в желудочковой системе головного мозга. Следовательно, жизненно важной становится ранняя диагностика, которая может быть выполнена с помощью компьютерной томографии (КТ), одного из наиболее эффективных методов диагностики гидроцефалии (КТ), при котором становится очевидным увеличение желудочковой системы. Однако большинство оценок прогрессирования заболевания основаны на оценке рентгенолога и физических показателях, которые являются субъективными, отнимающими много времени и неточными. В этой статье разрабатывается автоматическое прогнозирование с использованием фреймворка H-detect для повышения точности прогнозирования гидроцефалии. В этой статье используется этап предварительной обработки для нормализации входного изображения и удаления нежелательных шумов, что может помочь легко извлечь ценные признаки. Выделение признаков осуществляется путем сегментации изображения на основе определения границ с использованием треугольных нечетких правил. Таким образом, выделяется точная информация о природе ликвора внутри мозга. Эти сегментированные изображения сохраняются и снова передаются алгоритму CatBoost. Обработка категориальных признаков позволяет ускорить обучение. При необходимости детектор переобучения останавливает обучение модели и, таким образом, эффективно прогнозирует гидроцефалию. Результаты демонстрируют, что новая стратегия H-detect превосходит традиционные подходы.

Ключевые слова: гидроцефалия, компьютерная томография (КТ), метод H-детекции, спинномозговая жидкость (ликвор), треугольные нечеткие правила, обнаружение краев.

Литература

1. Zhang X.J., Guo J., Yang J. Cerebrospinal fluid biomarkers in idiopathic normal pressure hydrocephalus. Neuroimmunology and Neuroinflammation. 2020. vol. 7. no. 2. pp. 109–119.
2. Karimy J.K., Reeves B.C., Damisah E., Duy P.Q., Antwi P., David W., Kahle K.T. Inflammation in acquired Hydrocephalus: pathogenic mechanisms and therapeutic targets. Nature Reviews Neurology. 2020. vol. 16. no. 5. pp. 285–296.
3. Paulsen A.H. Adult outcome in pediatric Hydrocephalus. 2018. 58 p.
4. Saygili G., Yigin B.O., Guney G., Algin O. Exploiting lamina terminalis appearance and motion in the prediction of Hydrocephalus using convolutional LSTM network. Journal of Neuroradiology. 2022. vol. 49. no. 5. pp. 364–369.
5. Nakajima M., Kawamura K., Akiba C., Sakamoto K., Xu H., Kamohara C., Miyajima M. Differentiating comorbidities and predicting prognosis in idiopathic normal pressure hydrocephalus using cerebrospinal fluid biomarkers. Croatian Medical Journal. 2021. vol. 62. no. 4. pp. 387–398.

6. Yigin B.O., Algin O., Saygili G. Comparison of morphometric parameters in prediction of Hydrocephalus using random forests. Computers in Biology and Medicine. 2020. vol. 116. no. 103547.
7. Chiarelli P.A., Hauptman J.S., Browd S.R. Machine learning and the prediction of Hydrocephalus: Can quantitative image analysis assist the clinician? JAMA paediatric. 2018. vol. 172. no. 2. pp. 116–118.
8. Chen J., He W., Zhang X., Lv M., Zhou X., Yang X., Xia J. Value of MRI-based semi-quantitative structural neuroimaging in predicting the prognosis of patients with idiopathic normal pressure hydrocephalus after shunt surgery. European Radiology. 2022. vol. 32. no. 11. pp. 7800–7810.
9. Sotoudeh H., Sadaatpour Z., Rezaei A., Shafaat O., Sotoudeh E., Tabatabaie M., Tanwar M. The Role of Machine Learning and Radiomics for Treatment Response Prediction in Idiopathic Normal Pressure Hydrocephalus. Cureus. 2021. vol. 13. no. 10.
10. Mao Y., Shen Z., Wang J., Zhu H., Yu Z., Chen X., Cheng H. Deep Learning-Based MR Imaging for Analysis of Relation between Cerebrospinal Fluid Variation and Communicating Hydrocephalus after Decompressive Craniectomy for Craniocerebral Injury. Scientific Programming. 2022. vol. 2022.
11. Brito C., Machado A., Sousa A.L. Electrocardiogram beat classification based on a Res-Net network. Studies in Health Technology and Informatics. 2019. vol. 264. pp. 55–59.
12. Hu Y., Zhao H., Li W., Li J. Semantic image segmentation of brain MRI with deep learning. Zhong nan da XueXueBao. Yi Xue ban Journal of Central South University. Medical sciences. 2021. vol. 46. no. 8. pp. 858–864.
13. Kang J., Ullah Z., Gwak J. MRI-based brain tumour classification using ensemble of deep features and machine learning classifiers. Sensors. 2021. vol. 21(6). no. 2222.
14. Huang Y., Moreno R., Malani R., Meng A., Swinburne N., Holodny A.I., Young R.J. Deep Learning Achieves Neuroradiologist-Level Performance in Detecting Hydrocephalus Requiring Treatment. Journal of Digital Imaging. 2022. vol. 35. no. 6. pp. 1662–1672.
15. Narmatha C., Eljack S.M., Tuka A.A.R.M., Manimurugan S., Mustafa M. A hybrid fuzzy brain-storm optimization algorithm for the classification of brain tumour MRI images. Journal of ambient intelligence and humanized computing. 2020. pp. 1–9.
16. Prokhorenkova L., Gusev G., Vorobev A., Dorogush A.V, Gulin A. CatBoost: Unbiased Boosting with Categorical Features. Advances in Neural Information Processing Systems. 2018. vol. 31. pp. 6638–6648.
17. Nguyen N.Q., Lee S.W. Robust Boundary Segmentation in Medical Images Using a Consecutive Deep Encoder-Decoder Network. IEEE Access. 2019. vol. 7. pp. 33795–33808. DOI: 10.1109/ACCESS.2019.2904094.
18. Liu B., He S., He D., Zhang Y., Guizani M. A Spark-based Parallel Fuzzy c-Means Segmentation Algorithm for Agricultural Image Big Data. IEEE Access. 2019. vol. 7. pp. 42169–42180. DOI: 10.1109/ACCESS.2019.2907573.
19. Almotiri J., Elleithy K., Elleithy A. A Multi-Anatomical Retinal Structure Segmentation System for Automatic Eye Screening Using Morphological Adaptive Fuzzy Thresholding. IEEE Journal of Translational Engineering in Health and Medicine. 2018. vol. 6. pp. 1–23. DOI: 10.1109/JTEHM.2018.2835315.
20. Liu M., Jiang J., Wang Z. Colonic Polyp Detection in Endoscopic Videos with Single Shot Detection Based Deep Convolutional Neural Network. IEEE Access. 2019. vol. 7. pp. 75058–75066. DOI: 10.1109/ACCESS.2019.2921027.
21. Raweh A.A., Nassef M., Badr A. A Hybridized Feature Selection and Extraction Approach for Enhancing Cancer Prediction Based on DNA Methylation. IEEE Access. 2018. vol. 6. pp. 15212–15223. DOI: 10.1109/ACCESS.2018.2812734.

22. Gonzalez R., Tou J. Pattern recognition principles. Applied Mathematics and Computation. Reading, MA: Addison-Wesley. 1974. 377 p.
23. Lingras P., West C. Interval set clustering of web users with rough k-means. Journal of Intelligent Information Systems. 2004. vol. 23. no. 1. pp. 5–16. DOI: 10.1023/B:JIIS.0000029668.88665.1a.
24. Chuang K.S., Tzeng H.L., Chen S., Wu J., Chen T.J. Fuzzy c-means clustering with spatial information for image segmentation. Comput. Med. Imag. Graph., Jan. 2006. vol. 30. no. 1. pp. 9–15. DOI: 10.1016/j.compmedimag.2005.10.001.
25. Lingras P., Peters G. Applying rough set concepts to clustering. In Rough Sets: Selected Methods and Applications in Management and Engineering. London: Springer. 2012. pp. 23–37.
26. Ji Z., Sun Q., Xia Y., Chen Q., Xia D., Feng D. Generalized rough fuzzy c-means algorithm for brain MR image segmentation. Computer methods and programs in biomedicine. 2012. vol. 108. no. 2. pp. 644–655.
27. Namburu A., Srinivas Kumar S., Srinivasa Reddy E. Review of Set-Theoretic Approaches to Magnetic Resonance Brain Image Segmentation. IETE Journal of Research. 2022. vol. 68. no. 1. pp. 350–367. DOI: 10.1080/03772063.2019.1604176.
28. Dubey Y.K., Mushrif M.M., Mitra K. Segmentation of brain MR images using rough set based intuitionistic fuzzy clustering. Biocybern. Biomedical engineering. 2016. vol. 36. no. 2. pp. 413–426. DOI: 10.1016/j.bbe.2016.01.001.
29. Liu J., Peng Y., Zhang Y.A Fuzzy Reasoning Model for Cervical Intraepithelial Neoplasia Classification Using Temporal Grayscale Change and Textures of Cervical Images during Acetic Acid Tests. IEEE Access. 2019. vol. 7. pp. 13536–13545. DOI: 10.1109/ACCESS.2019.2893357.
30. Brunese L., Mercaldo F., Reginelli A., Santone A. Prostate Gleason Score Detection and Cancer Treatment through Real-Time Formal Verification. IEEE Access. 2019. vol. 7. pp. 186236–186246. DOI: 10.1109/ACCESS.2019.2961754.
31. Yin S., Zhang Y., Karim S. Large Scale Remote Sensing Image Segmentation Based on Fuzzy Region Competition and Gaussian Mixture Model. IEEE Access. 2018. vol. 6. pp. 26069–26080. DOI: 10.1109/ACCESS.2018.2834960.

Балони Дев — Ph.D., Dr.Sci., доцент, школа квантовых технологий, Университет Квантум. Область научных интересов: обработка изображений, машинное обучение, глубокое обучение, искусственный интеллект. Число научных публикаций — 20. devbaloni1982@gmail.com; шоссе Дехрадун, Мандавар, 247167, Рурки, Уттаракханд, Индия; р.т.: +91(8755)507-830.

Рай Дханвир Сингх — доцент, школа инженерии и вычислительной техники, Университет Дев Бхуми Уттаракханд. Область научных интересов: облачные вычисления, машинное обучение, глубокое обучение, искусственный интеллект. Число научных публикаций — 0. dhajvirrai123@gamil.com; Чакрата-роуд, Мандувала, 248007, Наагон, Уттаракханд, Индия; р.т.: +91(9557)891-499.

Сивагаминатан П.Г. — профессор, инженерная школа, Университет Аджинкья Д.Я. Патила. Область научных интересов: поиск информации, распознавание образов, искусственный интеллект, машинное обучение, глубокое обучение. Число научных публикаций — 31. sai.sivagaminathan@gmail.com; Городская дорога через Лохегаон, 412105, Чархоли Бадрек, Пуна, Махараштра, Индия; р.т.: +91(9500)903-614.

Анандарам Харишчандер — Ph.D., Dr.Sci., доцент, школа искусственного интеллекта "амрита", Амрита Вишва Видьяпитхам (Университет Амриты). Область научных интересов: биология вычислительных систем, функциональная геномика, биология

развития. Число научных публикаций — 43. a_harishchander@cb.amrita.edu; Амританагар, деревня Эттимадай, 641112, Коимбатур, Тамилнад, Индия; р.т.: +91(9940)066-227.

Таплиял Мадхур — доцент, Университет Graphic Era Hill. Область научных интересов: кибербезопасность, обработка изображений, глубокое обучение, машинное обучение. Число научных публикаций — 3. madhurthapliyal@gehu.ac.in; Белл-роуд, Клемент-Таун, 248002, Дехрадун, Уттаракханд, Индия; р.т.: +91(7017)747-897.

Джоши Капил — Ph.D., Dr.Sci., доцент, технологический институт уттаранчала, Университет Уттаранчала. Область научных интересов: слияние изображений, обработка изображений, глубокое обучение, CNN. Число научных публикаций — 132. Kapilengg0509@gmail.com; Прем Нагар, 248007, Дехрадун, Уттаракханд, Россия; р.т.: +91(8979)799-289.